



## Evidence from detrital zircons for recycling of Mesoproterozoic and Neoproterozoic crust recorded in Paleozoic and Mesozoic sandstones of southern Libya

Guido Meinhold <sup>a,b,\*</sup>, Andrew C. Morton <sup>a,c</sup>, C. Mark Fanning <sup>d</sup>, Dirk Frei <sup>e,f</sup>, James P. Howard <sup>a</sup>, Richard J. Phillips <sup>a,g</sup>, Dominic Strogon <sup>a,h</sup>, Andrew G. Whitham <sup>a</sup>

<sup>a</sup> CASP, University of Cambridge, West Building, 181A Huntingdon Road, Cambridge CB3 0DH, United Kingdom

<sup>b</sup> Department of Sedimentology & Environmental Geology, Geoscience Centre, University of Göttingen, Goldschmidtstraße 3, 37077 Göttingen, Germany

<sup>c</sup> HM Research Associates, 2 Clive Road, Balsall Common CV7 7DW, United Kingdom

<sup>d</sup> Research School of Earth Sciences, Australian National University, Canberra ACT 0200, Australia

<sup>e</sup> Geological Survey of Denmark and Greenland (GEUS), Øster Voldgade 10, DK-1350 Copenhagen, Denmark

<sup>f</sup> Department of Earth Sciences, Stellenbosch University, Private Bag X1, Matieland 7602, South Africa

<sup>g</sup> School of Earth and Environment, University of Leeds, Leeds LS2 9JT, United Kingdom

<sup>h</sup> GNS Science, P.O. Box 30368, Lower Hutt 5010, New Zealand

### ARTICLE INFO

#### Article history:

Received 7 July 2011

Received in revised form 28 September 2011

Accepted 29 September 2011

Available online 1 November 2011

Editor: T.M. Harrison

#### Keywords:

zircon U–Pb ages  
sediment provenance  
Mesoproterozoic  
Paleozoic  
northern Gondwana  
Libya

### ABSTRACT

The geodynamic history of the Precambrian basement in central North Africa as well as the age and provenance of its sedimentary cover sequence are still poorly constrained. Here we present first detrital zircon ages (obtained by LA-SF-ICP-MS and SHRIMP) from Paleozoic and Mesozoic sandstones of the eastern Murzuq Basin, southern Libya, which unconformably overlie the Saharan Metacraton. Establishing the age and provenance of these sandstones has important implications for our understanding of the evolution of northern Gondwana during the Paleozoic, especially for reconstructions of paleo-source areas and transport paths. Detrital zircons from the sandstones show mainly early Paleozoic to Neoproterozoic ages with four main age populations, at 2750–2500 Ma (8%), 2200–1750 Ma (16%), 1060–920 Ma (18%), and 720–530 Ma (39%). About 13% of all concordant grains yield ages of 1600–1000 Ma. In addition, there are 9 zircon grains (0.7% of all concordant grains) with ages of 3600–2800 Ma. The presence of a high number of ca. 1 Ga zircons is enigmatic and their origin is controversial. Besides direct sourcing from ca. 1 Ga igneous rocks in eastern Chad and ca. 1 Ga igneous rocks along the southeastern margins of the Congo and Tanzania cratons, recycling of Neoproterozoic sediments containing ca. 1 Ga zircons is another alternative hypothesis to explain the presence of ca. 1 Ga zircons in the Paleozoic sedimentary sequence of central North Africa. The ubiquitous occurrence of ca. 1 Ga zircons in Paleozoic sediments of southern Libya provides insights into the correlation and paleotectonic arrangement of Gondwana-derived terranes, present, for example, in the eastern Mediterranean and in southwestern Europe. Current paleotectonic models of dextral terrane transport along the northern Gondwana margin during the early Paleozoic may need to be revised.

© 2011 Elsevier B.V. All rights reserved.

### 1. Introduction

An area built of Precambrian igneous, sedimentary and metamorphic rocks largely covered by a thick pile of Paleozoic and younger sedimentary rocks extends for more than 6000 km from the Atlantic coast of North Africa to the east coast of the Arabian peninsula (e.g., Burke et al., 2003). The assembly of North Africa was related to a number of orogenic cycles, which lasted from ca. 900 to 550 Ma (e.g., Abdelsalam et al., 2002; Collins and Pisarevsky, 2005; Johnson et al., 2011; Küster et al., 2008; Stern, 1994). The central part of

North Africa, which comprises a heterogeneous mixture of Archean, Paleo-, Meso- and Neoproterozoic rocks with old continental as well as juvenile isotopic signatures, is commonly referred to as the Saharan Metacraton (Abdelsalam et al., 2002, 2011) or sometimes as the Eastern Saharan Craton (Bertrand and Caby, 1978) or Central Saharan Ghost Craton (Black and Liégeois, 1993). The Saharan Metacraton (SMC) is bordered by the Hoggar to the west, the Congo Craton to the south, and the Arabian–Nubian Shield (ANS) to the east (Fig. 1). Because large parts are covered by Paleozoic and younger sediments the geodynamic history of the SMC is still poorly constrained. Abdelsalam et al. (2011) presented new insights into the sub-continental lithospheric mantle of the SMC using S-wave velocity data. They suggested that widespread emplacement of high-K calc-alkaline granitoids and migmatization at ca. 600 Ma might be due to mantle delamination or convective removal during the

\* Corresponding author at: Department of Sedimentology & Environmental Geology, Geoscience Centre, University of Göttingen, Goldschmidtstraße 3, 37077 Göttingen, Germany. Tel.: +49 551 393455; fax: +49 551 397996.

E-mail address: [variscides@gmail.com](mailto:variscides@gmail.com) (G. Meinhold).

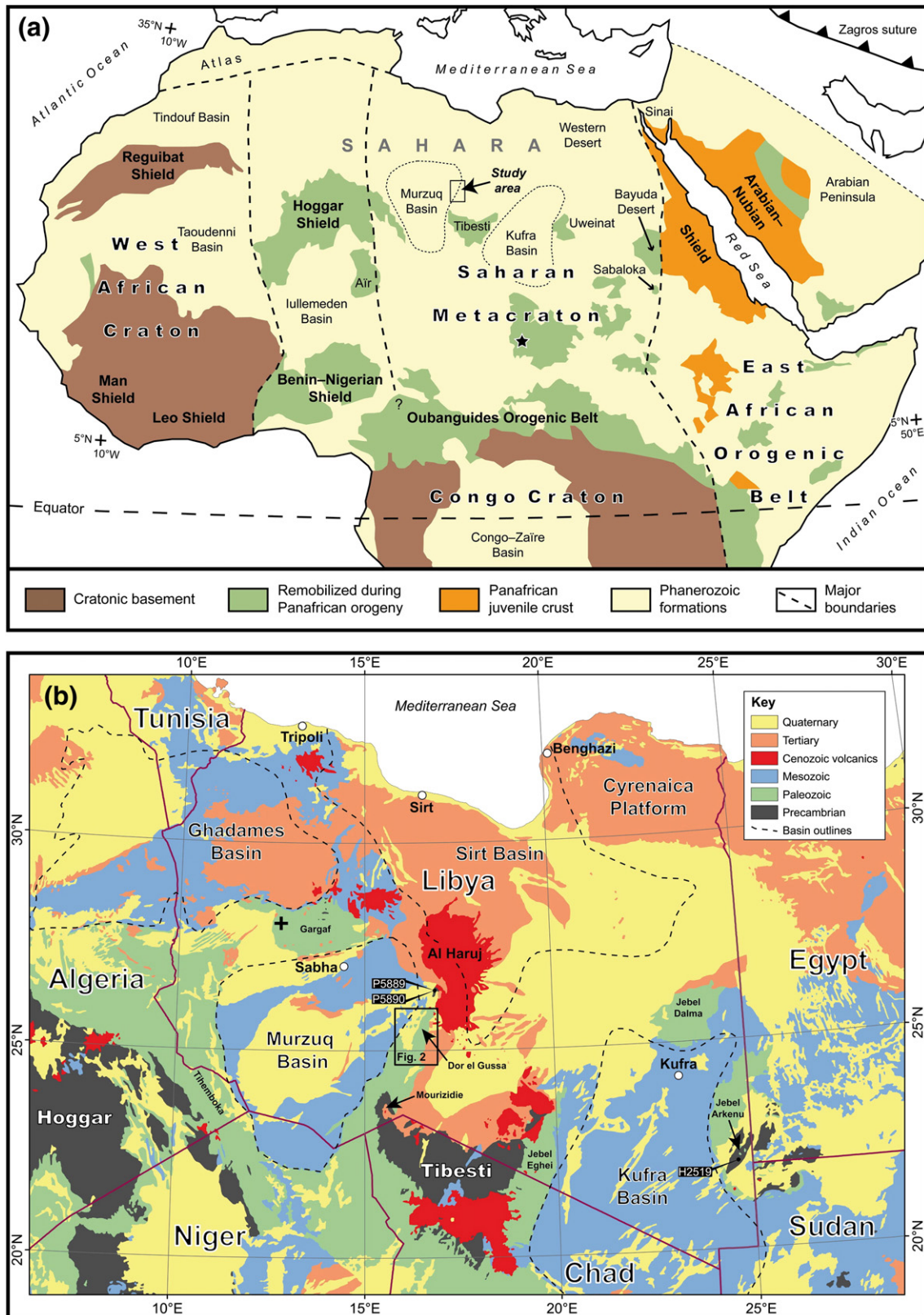


**Fig. 1.** (a) Map of North Africa showing exposures of Precambrian rocks and major tectonic units (compiled from Abdelsalam et al., 2002; Avigad et al., 2003; Key, 1992; Kolodner et al., 2006; Küster et al., 2008). The black star denotes the region in western Dharfur (eastern Chad) from which de Wit et al. (2005) reported extensive ca. 900 and ca. 600 Ma granitoids, predominantly derived from melting of 3.0–1.0 Ga continental lithosphere. (b) Geological map of Libya and neighbouring countries (after Persits et al., 2002) showing location of the Dor el Gussa region at the eastern margin of the Murzuq Basin. Basin outlines (after Boote et al., 1998) are shown as dashed lines. The black cross denotes the location in western Gargaf from which Ramos et al. (2003, 2006) reported several K-bentonite beds within the Middle Ordovician Hawaz Formation. A close up of the Dor el Gussa region is shown in Fig. 2. The location of two samples (P5889 and P5890) collected from north of Dor el Gussa and of the Arkenu Formation sample H2519 (Le Heron et al., 2009) is also indicated.

Neoproterozoic. Furthermore, the structure of the SMC had a strong influence on Phanerozoic events (Abdelsalam et al., 2011).

Understanding the tectonic events and sedimentary cover sequence is fundamental for better understanding the origin of the SMC and its Phanerozoic history. The more marginal parts of the SMC, exposed in Egypt, Sudan, Chad, Niger and western Algeria have already been studied in some detail (e.g., Abdelsalam et al., 2002; Küster et al., 2008, and references therein). The central part of the SMC, covering Libya, however, is still lacking a detailed study. The present study focuses on the Paleozoic cover sequence rather than the Precambrian basement. In Libya, exposures of Paleozoic rocks are found along the margins of the Kufra and Murzuq basins (Fig. 2). Paleozoic strata of the Murzuq Basin host large hydrocarbon reserves (e.g., Aziz, 2000; Boote et al., 1998; Craig et al., 2008; Davidson et al., 2000; Hallett, 2002) which make it attractive to international oil and gas companies, providing the impetus for field-based research in southern Libya. Although the centre of the Murzuq Basin has been extensively studied in recent years by seismic and borehole data, the margins of this basin, especially the eastern margin, need studies focused on understanding their provenance and depositional history.

In the present study, we applied sensitive high-resolution ion microprobe (SHRIMP) and high-spatial resolution laser ablation sector-

field inductively coupled plasma mass spectrometry (LA-SF-ICP-MS) to determine U–Pb ages of detrital zircon grains from Paleozoic and Mesozoic sandstones of the eastern Murzuq Basin (Figs. 2 and 3). The study of clastic sediments is crucial for paleotectonic reconstructions because they can provide information about potential lithologies in the source area, which have commonly been destroyed and recycled during ancient plate tectonic processes. Furthermore, in the absence of fossil and other stratigraphic data, the youngest grains (e.g., zircon) in a sedimentary rock can indicate a maximum depositional age (e.g., Fedo et al., 2003; Meinhold and Frei, 2008). This is important because the Paleozoic succession of southern Libya consists of substantial thicknesses of non-marine to shallow marine sandstones that are poorly dated due to the lack of body fossils, the exception being fossiliferous clastic sediments of Carboniferous age (e.g., Klitzsch, 1964; Klitzsch and Ziegert, 2000). Understanding the age and origin of these sedimentary units is important for reconstructions of paleosource areas and sediment transport and may give novel approaches to test current plate tectonic models, with important implications for our understanding of the evolution of northern Gondwana during the Paleozoic.

## 2. Geological setting

The Murzuq Basin covers an area of about 350,000 km<sup>2</sup> and is located in the southwest of Libya, and continues into northwestern Chad, northern Niger and eastern Algeria (e.g., Boote et al., 1998; Davidson et al., 2000) (Fig. 1). Its present-day sedimentary fill reaches a maximum thickness of about 4000 m in the basin centre (Davidson et al., 2000). The present-day eastern margin of the Murzuq Basin, the Dor el Gussa region, is the focus of this study. This area is dominated by a clastic sedimentary sequence of Cambrian to Carboniferous age (Klitzsch, 1964; Klitzsch and Ziegert, 2000) (Fig. 2). Precambrian basement is exposed to the north and south of Dor el Gussa and comprises metasedimentary and igneous rocks. The latter are mainly granites, granodiorites and diorites, with minor amounts of gabbro and quartz monzonites (Baumann et al., 1992; Pegram et al., 1976) of a typical calcalkaline suite (Ghuma and Rogers, 1978). Isotopic studies yielded ages of ca. 586–533 Ma (Rb–Sr method; Pegram et al., 1976) for granites, pegmatites and gabbros south of Dor el Gussa and ca. 554–551 Ma (Rb–Sr method; Baumann et al., 1992) for granites north of Dor el Gussa.

Dor el Gussa belongs to one of the least geologically studied areas in Libya and only a limited number of publications are available, illustrating the need for further geoscientific research. The oldest Paleozoic strata exposed in Dor el Gussa belong to the Cambrian (ca. 542–488 Ma) Hasawnah Formation, which unconformably overlies Ediacaran–Cambrian basement north of Dor el Gussa (Klitzsch, 1964; Klitzsch and Ziegert, 2000). The Hasawnah Formation consists of medium- to very coarse-grained, commonly cross-laminated, feldspar-bearing sandstones (Klitzsch, 1964). The thickness of the Hasawnah Formation varies from 600 to 1700 m in the northern part of Dor el Gussa (Hallett, 2002; Klitzsch, 1964) to 300–400 m to the south of Dor el Gussa, in the Mourizidie area (Hallett, 2002). The Middle Ordovician (ca. 472–461 Ma) Hawaz Formation (≤50 m thick) unconformably overlies the Hasawnah Formation and consists of very fine- to medium-grained sandstone, thin- to thick-bedded and well sorted (Aziz, 2000; El-Hawat et al., 2003; Hallett, 2002; Klitzsch and Ziegert, 2000). *Skolithos*-bearing sandstone is common in the Hawaz Formation (e.g., De Gibert et al., 2011; Hallett, 2002; Klitzsch, 1964; Klitzsch and Ziegert, 2000; Ramos et al., 2006). Palynological studies on subsurface samples suggest that the Hawaz Formation is Darriwilian (ca. 468–461 Ma) in age (Abuhmida, 2011; Ramos et al., 2006) and probably includes the base of the Late Ordovician (Ramos et al., 2006).

The Cambrian to Middle Ordovician sediments show a transitional environment from continental to shallow marine. The Hawaz

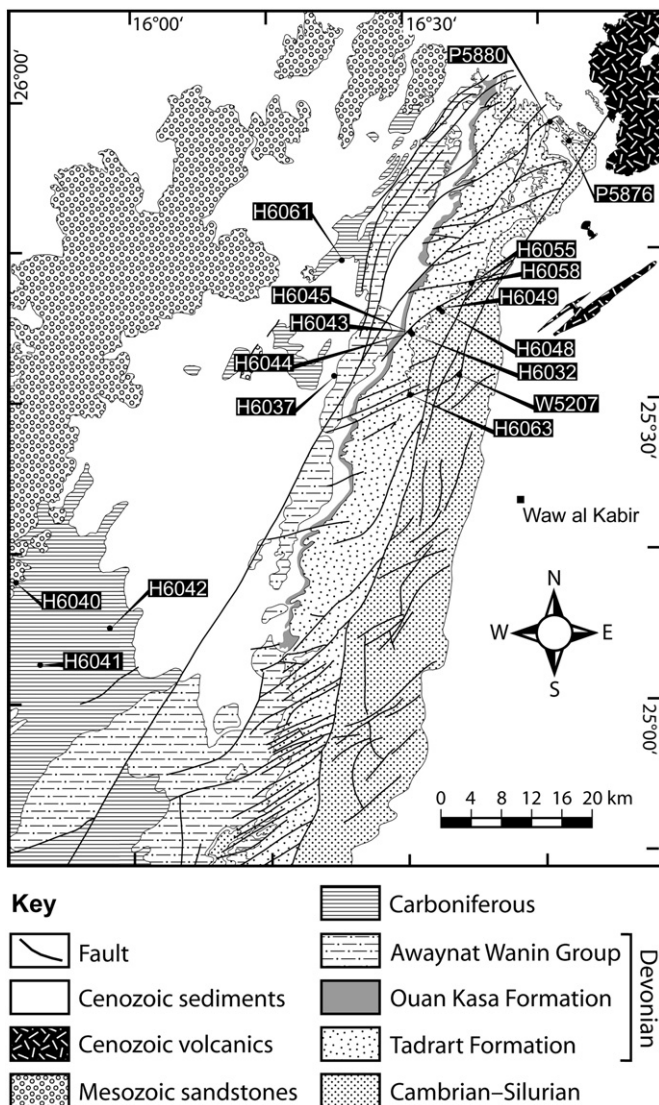
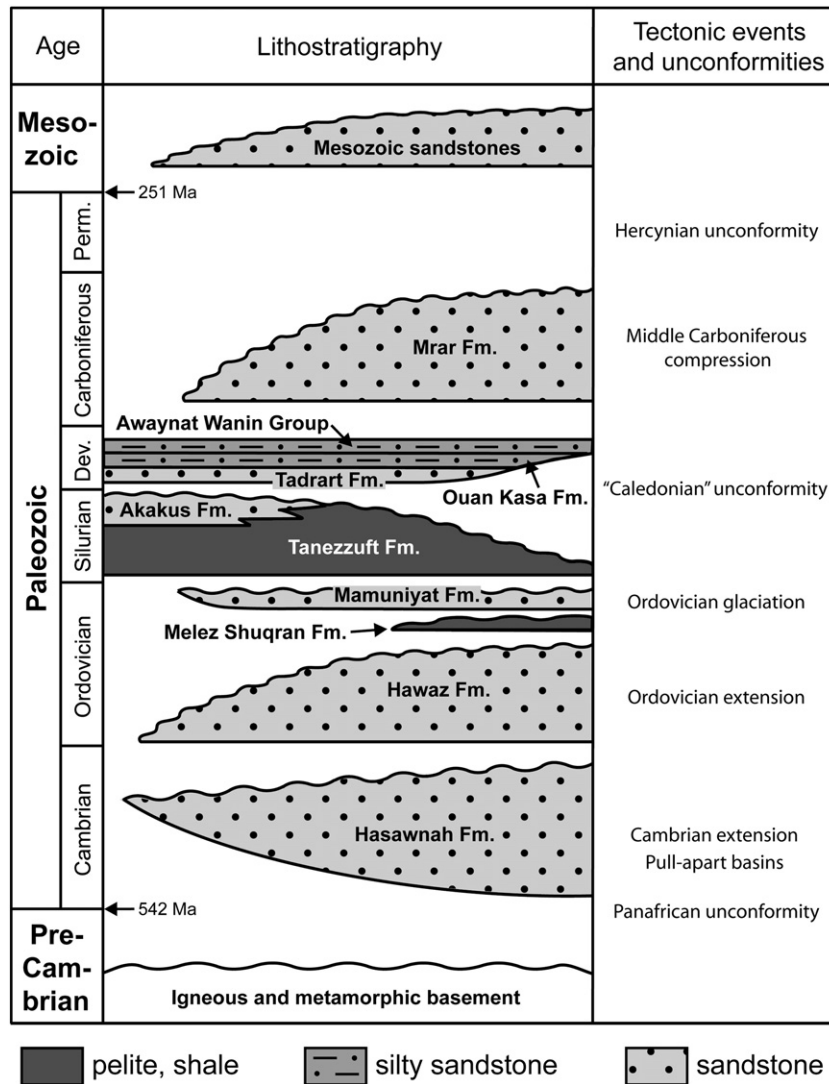


Fig. 2. Simplified geologic map of the Dor el Gussa region (after Collomb, 1962) showing the location of analysed samples.



**Fig. 3.** Stratigraphic chart for the Dor el Gussa region and major tectonic events recorded in the Murzuq Basin (compiled from Klitzsch, 1964; Klitzsch and Ziegert, 2000; Ramos et al., 2006). Because of uncertain stratigraphy the term Mesozoic sandstones is used here for all Mesozoic-aged sediments.

Formation is unconformably overlain by the Late Ordovician Melez Shuqran Formation ( $\leq 25$  m thick), which is of limited extent and consists of silty to sandy, grey and red shale, with many intercalated fine-grained sandstone beds (El-Hawat et al., 2003; Klitzsch and Ziegert, 2000). Palynological studies on subsurface samples from the Murzuq Basin suggest that the Melez Shuqran Formation is late Katian to early Hirnantian (ca. 450–445 Ma) in age (Abuhmida, 2011). McDougall and Martin (2000) mentioned the occurrences of dropstones. The Melez Shuqran Formation (if present) is overlain by the Hirnantian (ca. 446–444 Ma) Mamuniyat Formation ( $\leq 30$  m thick), probably with a stratigraphic break (Klitzsch, 1964). The Mamuniyat Formation is predominantly composed of massive, fine- to coarse-grained, in parts conglomeratic, commonly tabular cross-bedded sandstone (e.g., Aziz, 2000; Klitzsch, 1964; Klitzsch and Ziegert, 2000). Soft-sediment deformation structures within the Mamuniyat Formation are attributed to glaciotectionic processes related to the late Ordovician (Hirnantian) glaciation (e.g., Le Heron et al., 2005).

The Mamuniyat Formation is transgressively overlain by the early Silurian (ca. 444–428 Ma) Tanezzuft Formation (40–160 m thick). This formation (when unweathered) consists of dark grey shale, very compact, commonly with mica and pyrite, locally with silty and fine-grained sandy interlaminae and beds (Aziz, 2000; Hallett,

2002; Klitzsch, 1964). The transition from the Tanezzuft Formation into the overlying early-late Silurian (~436–416 Ma) Akakus Formation is gradual, with an increase in the sandy component (Hallett, 2002; Klitzsch, 1964). In many places, it is not possible to separate the two formations. The Akakus Formation ( $\leq 465$  m thick) consists of fine- to medium-grained silty sandstones, white to grey, thinly bedded, commonly cross-bedded, with ripple and flute marks (Klitzsch, 1964; Klitzsch and Ziegert, 2000).

The oldest Devonian strata belong to the Tadrart Formation ( $\leq 415$  m thick), which consists of massive sandstone, fine-grained to slightly conglomeratic, thick-bedded, cross-stratified, very ferruginous in some beds, but normally without matrix and very friable, deposited in a fluvial environment (Klitzsch, 1964). In eastern Dor el Gussa, the Tadrart Formation rests with an unconformity of 3–5° on the middle part of the Tanezzuft Formation. The Tadrart Formation is conformably overlain towards the west by the Ouan Kasa Formation (70–120 m thick), which consists of shale and silty shale alternating with fine-grained sandstone and calcareous siltstone (Klitzsch, 1964; Klitzsch and Ziegert, 2000).

Recent observations made during CASP fieldwork and paleobotanical studies (unpublished CASP data) suggest that in central and northern Dor el Gussa the Tadrart and Ouan Kasa formation sediments may be of Middle to early Late Devonian age (ca. 397–

374 Ma). There is a gradual transition from the Tadrart Formation to the Ouan Kasa Formation, which itself is unconformably overlain by the Awaynat Wanin Group (140–310 m thick). The Awaynat Wanin Group (also spelt “Aouinet Ouenine Group”) consists of fine-grained, thin- to partly thick-bedded sandstone intercalated with silty shale layers up to 10 m thick. In the eastern Murzuq Basin, the upper part of the Awaynat Wanin Group is missing (Klitzsch and Ziegert, 2000). Analysis of brachiopod fauna suggests a Middle to Late Devonian (Eifelian to Famennian) age for the Awaynat Wanin Group in its type area (Mergl and Massa, 2000).

The Awaynat Wanin Group is unconformably overlain by early Carboniferous (ca. 359–318 Ma) sediments of the Mrar Formation (<1000 m thick) (Klitzsch and Ziegert, 2000). In many places along the western flank of Dor el Gussa, the base of the Mrar Formation is marked by a 1-m-thick conglomeratic sandstone bed overlain by <120 m of partly silty, grey-green or black shale (Klitzsch, 1964; Klitzsch and Ziegert, 2000). The succession is overlain by a further 250 m of interbedded sandstone and shale, with an increase in the sandstone component towards northwest Dor el Gussa.

The youngest strata investigated in this study belong to the Post-Tassilian and Nubian Series (<200 m thick) of probable Triassic–early Cretaceous age (Klitzsch, 1964). At the eastern margin of the Murzuq Basin, the Post-Tassilian is subdivided into the Unar and Messak formations (Klitzsch and Ziegert, 2000). We use here the simplified term Mesozoic sandstones, describing sandstones that unconformably overlie Carboniferous and older strata. The Mesozoic sandstones are varicoloured (typically reddish, yellowish, purplish and brownish) quartzose, cross-bedded and pebbly, with interbeds of conglomerate, siltstone and mudstone. Further details about the stratigraphy of the eastern Murzuq Basin can be found in Klitzsch (1964), Klitzsch and Ziegert (2000) and Hallett (2002).

### 3. Sample preparation and analytical techniques

Sample preparation and analytical procedures for U–Pb isotopic analyses are reported in Appendix A. Altogether 19 samples were analysed for U–Pb detrital zircon dating. A list of samples and a summary

of analysed grains per sample are given in Table 1. The U–Pb isotopic data are given as Supplementary data (see Appendix B).

### 4. Results

In total 1678 zircon ages have been obtained from 19 sandstone samples of the eastern Murzuq Basin, of which 1257 grains (75% of all zircons) are 90–110% concordant (Table 1). Information about data interpretation and illustration is reported in Appendix A. Histograms (Fig. 5) show combined sets of U–Pb analytical zircon data for analysed Paleozoic and Mesozoic sandstone samples. Histograms and probability density curves for each single sandstone sample analysed in this study are given as Supplementary data (see Appendix B).

#### 4.1. Hasawnah Formation (Cambrian)

In total, 336 zircons from four Hasawnah Formation sandstone samples have been analysed, of which 243 provided reliable data for interpretation (Table 1; Fig. 5). Two samples (P5889, P5890) were collected from exposures north of Dor el Gussa, close to the Al Haruj volcanic field (Fig. 1b). These samples contain abundant zircon grains with high levels of common Pb, which resulted in unreliable ages. Thus, 43 of the 94 analysed grains (46%) from sample P5890 and 42 of the 102 analysed grains (41%) from sample P5889 gave discordances of >10% and had to be rejected. Extensive fluid circulation related to Cenozoic volcanic activity is the most plausible explanation for disturbance of the isotopic system in the zircon crystals. The third sample (P5876) was collected further away from the Al Haruj volcanic field, at the unconformity between the Cambrian and the Ordovician in northern Dor el Gussa (El-Hawat et al., 2003; Klitzsch, 1964). In this sample, 67 of the 70 analyses (96%) could be used for interpretation.

Between 62% and 77% of the zircons from the four Hasawnah Formation samples have Neoproterozoic ages (between 1000 and 542 Ma), the majority being between 720 and 530 Ma (Late Cryogenian–Early Cambrian). Samples P5890 and P5889 also contain a number of zircons with ages between 1060 and 920 Ma (22% and

**Table 1**  
Sample information. (First six columns) Location of samples analysed in this study. Note, based on CASP fieldwork and paleobotanical studies on vascular plant fossils from the eastern Murzuq Basin, the age of the Tadrart and Ouan Kasa formations has been revised from Early Devonian to Middle–Late Devonian. The samples analysed in this study are quartz arenites and minor arkosic arenites with zircon, tourmaline and rutile as main heavy minerals (see Fig. 4). (Last four columns) Summary of detrital zircon ages of samples analysed in this study. The full data set is given as Supplementary data (see Appendix B).

Sample name	Latitude	Longitude	Age	Stratigraphy	Rock type	Method	Number of determined ages	Number of concordant ages	Number of concordant ages in %
H6040	25° 12' 1.44"	15° 46' 33.15"	Triassic–early Cretaceous	Mesozoic sandstones	Quartz arenite	SHRIMP	70	62	89
H6037	25° 32' 35.99"	16° 21' 46.11"	Carboniferous	Mrar Formation	Arkosic arenite	LA-ICP-MS	24	10	42
H6041	25° 3' 47.44"	15° 49' 9.69"	Carboniferous	Mrar Formation	Arkosic arenite	LA-ICP-MS	17	8	47
H6042	25° 7' 25.78"	15° 57' 37.97"	Carboniferous	Mrar Formation	Arkosic arenite	SHRIMP	65	58	89
H6061	25° 43' 51.5"	16° 23' 23.09"	Carboniferous	Mrar Formation	Arkosic arenite	LA-ICP-MS	120	79	66
H6043	25° 36' 37.57"	16° 30' 21.45"	Middle–Late Devonian	Awaynat Wanin Group	Quartz arenite	SHRIMP	67	63	94
H6044	25° 36' 37.57"	16° 30' 21.45"	Middle–Late Devonian	Awaynat Wanin Group	Quartz arenite	LA-ICP-MS	120	91	76
H6032	25° 36' 20.35"	16° 30' 40.67"	Middle–Late Devonian	Tadrart Formation	Quartz arenite	SHRIMP	71	61	86
H6045	25° 36' 46.39"	16° 30' 22.71"	Middle–Late Devonian	Tadrart Formation	Quartz arenite	LA-ICP-MS	120	88	73
H6049	25° 39' 5.58"	16° 33' 47.83"	Middle–Late Devonian	Tadrart Formation	Quartz arenite	SHRIMP	66	58	88
H6055	25° 41' 27.41"	16° 37' 8.4"	Middle–Late Devonian	Tadrart Formation	Quartz arenite	LA-ICP-MS	122	101	83
H6058	25° 41' 27.41"	16° 37' 8.4"	early Silurian	Tanezzuft Formation	Arkosic arenite	LA-ICP-MS	120	99	83
P5880	25° 57' 49.5"	16° 46' 36.77"	Middle Ordovician	Hawaz Formation	Quartz arenite	LA-ICP-MS	120	70	58
H6048	25° 38' 32.26"	16° 34' 15.15"	Middle Ordovician	Hawaz Formation	Quartz arenite	LA-ICP-MS	120	96	80
H6063	25° 30' 9.4"	16° 30' 42.1"	Middle Ordovician	Hawaz Formation	Quartz arenite	LA-ICP-MS	120	70	58
W5207	25° 32' 12.94"	16° 35' 53.13"	Cambrian	Hasawnah Formation	Quartz arenite	SHRIMP	70	65	93
P5876	25° 55' 49.8"	16° 48' 33.41"	Cambrian	Hasawnah Formation	Quartz arenite	SHRIMP	70	67	96
P5889	26° 29' 31.31"	16° 50' 21.48"	Cambrian	Hasawnah Formation	Quartz arenite	LA-ICP-MS	102	60	59
P5890	26° 29' 31.31"	16° 50' 21.48"	Cambrian	Hasawnah Formation	Quartz arenite	LA-ICP-MS	94	51	54
						Total:	1678	1257	
							100%	75%	

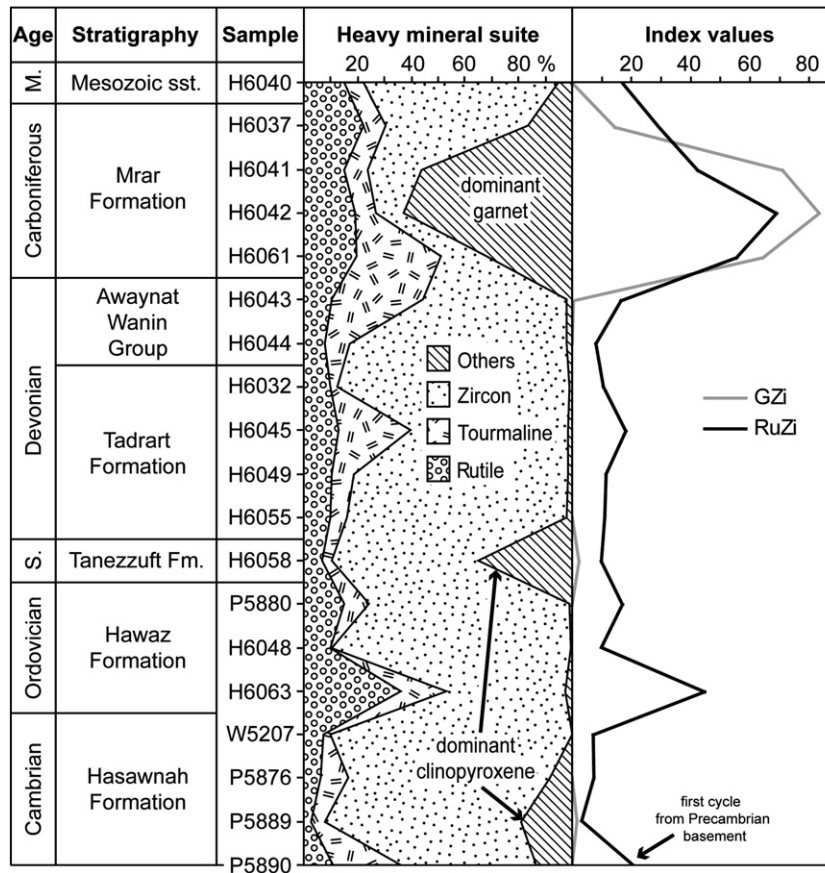


**Fig. 4.** Stratigraphic variations in zircon, tourmaline, rutile and other heavy mineral abundance, and index values GZi (garnet:zircon) and RuZi (rutile:zircon) in sandstones analysed in this study (data were taken from Morton et al., 2011). Most of the heavy mineral assemblages are limited in diversity, being dominated by zircon, tourmaline and rutile. Although clinopyroxene abundances may have been modified to some degree by weathering at outcrop, variations in clinopyroxene abundance appear to have stratigraphic significance. Garnet:zircon (GZi) and rutile:zircon (RuZi) values are at their highest in the youngest parts of the succession (Mrar Formation and Mesozoic sandstones).

14% respectively). All samples also have some 2500–1600 Ma (6–17%) and 3600–2500 Ma (1–8%) zircons. The oldest zircon grain of the Hasawnah Formation comes from sample W5207 and is  $3451 \pm 10$  Ma-old. The youngest concordant zircon grains have ages of  $518 \pm 12$  Ma and  $498 \pm 6$  Ma in sample W5207 and  $484 \pm 10$  Ma and  $478 \pm 10$  Ma in sample P5876, giving maximum ages of deposition for the Hasawnah Formation samples. The two youngest zircon grains from sample P5876 suggest that in northern Dor el Gussa, the upper part of the Hasawnah Formation may be younger than Cambrian since the Cambrian/Ordovician boundary is at ca. 488 Ma (Ogg et al., 2008).

#### 4.2. Hawaz Formation (middle Ordovician)

In total, 360 zircons from three sandstone samples within the Hawaz Formation have been analysed, of which 236 have been used for interpretation (Table 1; Fig. 5). Samples H6063, H6048 and P5880 show similar zircon spectra, with major populations at 2200–1750 Ma (16–34%), 1160–920 Ma (19–26%) and 720–530 Ma (19–40%). A Neoproterozoic zircon population of 2750–2500 Ma (5–9%) is also present, but compared with the other zircon populations it is of minor significance. Worthy of mention is a single grain of Paleoproterozoic age ( $3570 \pm 23$  Ma) from sample H6048, with a concordance of 98%, which is the oldest zircon grain from all analysed Libyan samples so far (see also Appendix B). The youngest concordant zircon grains have ages of  $507 \pm 9$  Ma in sample H6048,  $464 \pm 17$  Ma in sample H6063, and  $461 \pm 23$  Ma in sample P5880, giving maximum ages of deposition for the Hawaz Formation samples.

#### 4.3. Tanezzuft Formation (early Silurian)

In total, 120 zircons from sample H6058 from the Tanezzuft Formation have been analysed, of which 99 have been used for interpretation (Table 1; Fig. 5). About 40% of the zircon grains are between 720 and 530 Ma in age; minor populations are at 2200–1750 Ma (22%) and 1160–920 Ma (13%). The youngest concordant zircon grain is  $481 \pm 14$  Ma and the oldest zircon grain is  $2720 \pm 51$  Ma.

#### 4.4. Tadrart Formation (Middle to Late Devonian)

In total, 379 zircons from four samples from the Tadrart Formation have been analysed, of which 308 have been used for interpretation (Table 1; Fig. 5). Samples H6055, H6049, H6045 and H6032 have very similar zircon spectra, with major populations at 2750–2500 Ma (8–13%), 2200–1750 Ma (10–22%), 1060–920 Ma (20–24%), and 720–530 Ma (26–43%). The youngest concordant zircon grains have ages of  $497 \pm 17$  Ma in sample H6055,  $485 \pm 10$  Ma in sample H6049,  $491 \pm 16$  Ma in sample H6045 and  $506 \pm 13$  Ma in sample H6032. The oldest zircon grain of the Tadrart Formation comes from sample H6055 and is  $3153 \pm 46$  Ma.

#### 4.5. Awaynat Wanin Group (Middle to Late Devonian)

In total, 187 zircons from two samples from the Awaynat Wanin Group have been analysed, of which 154 have been used for interpretation (Table 1; Fig. 5). Both samples (H6043 and H6044) have major populations at 2750–2500 Ma (3 and 8%), 2200–1750 Ma (22 and 16%), 1060–

920 Ma (41 and 16%) and 720–530 Ma (29 and 42%). The youngest concordant zircon grains have ages of  $498 \pm 12$  Ma in sample H6043 and  $530 \pm 13$  Ma in sample H6044. The oldest zircon grain of the Awaynat Wanin Group comes from sample H6044 and is  $3416 \pm 37$  Ma.

#### 4.6. Mrar Formation (Carboniferous)

In total, 226 zircons from four samples from the Mrar Formation have been analysed, of which 155 are 90 to 110% concordant. Two samples (H6037 and H6041) contained only a small quantity of zircons for picking and thus yielded only very few grains for U–Pb zircon dating (less than 25; Table 1). Moreover, many zircon grains from these samples have high amounts of common Pb, which resulted in unreliable ages. Less than 50% of the determined ages were reliable. These samples have carbonaceous material as matrix, which makes them more susceptible to fluid circulation, and this may explain the high amount of common Pb. From the remaining samples H6061 and H6042, 66% and 89% of the determined ages were reliable (Table 1). Samples from the Mrar Formation show some additional zircon age populations (10% and 6% of the zircon grains have ages of 720–810 Ma and <530 Ma respectively) compared with all other samples. Nonetheless, in all Mrar Formation samples major populations are recorded at 2750–2500 Ma (8%), 2200–1750 Ma (12%), 1060–920 Ma (15%) and 720–530 Ma (36%). The youngest and oldest concordant zircon grains come from sample H6061 with ages of  $459 \pm 15$  Ma and  $2952 \pm 31$  Ma respectively.

#### 4.7. Mesozoic sandstones

In total, 70 zircons from Mesozoic sandstone sample H6040 have been analysed, of which 62 are 90 to 110% concordant (Table 1). About 60% of the zircon grains give Neoproterozoic ages and 18% are Mesoproterozoic in age. The major zircon populations are recorded at 2750–2500 Ma (8%), 2200–1750 Ma (11%), 1060–920 Ma (23%) and 720–530 Ma (52%). The youngest concordant zircon grain is  $519 \pm 17$  Ma and the oldest grain is  $2693 \pm 26$  Ma. Fig. 6 shows relative abundances of detrital zircons from all stratigraphic units for comparison.

### 5. Discussion

In most samples, the zircon populations are similar, the only differences being due to variations in the relative abundance of the four main age groups (Figs. 5 and 6). These are at 2750–2500 Ma (8%), 2200–1750 Ma (16%), 1060–920 Ma (18%), and 720–530 Ma (39%). About 13% of all concordant grains yield ages of 1600–1000 Ma, which are ubiquitous in the Middle Ordovician Hawaz Formation and younger sandstones. In addition, 0.7% of all concordant grains yield ages of 3600–2800 Ma.

The Cryogenian–Ediacaran group represents orogenic events associated with the assembly of northern Gondwana (e.g., Abdelsalam et al., 2002; Black and Liégeois, 1993; Collins and Pisarevsky, 2005; Johnson et al., 2011; Kröner et al., 1987; Küster et al., 2008; Stern, 1994). The few early Paleozoic ages (ca. 510–460 Ma) reported, for example, in samples from the Middle Ordovician Hawaz and the Carboniferous Mrar formations (Fig. 5), are probably related to post-orogenic alkaline magmatism (Hohndorf et al., 1994; Veevers, 2007). The Saharan Metacraton (SMC) is considered to be the most likely source for the Neoproterozoic zircons because basement of such age is recognised within it (e.g., Abdelsalam et al., 2002; Baumann et al., 1992; Pegram et al., 1976, and references therein). The

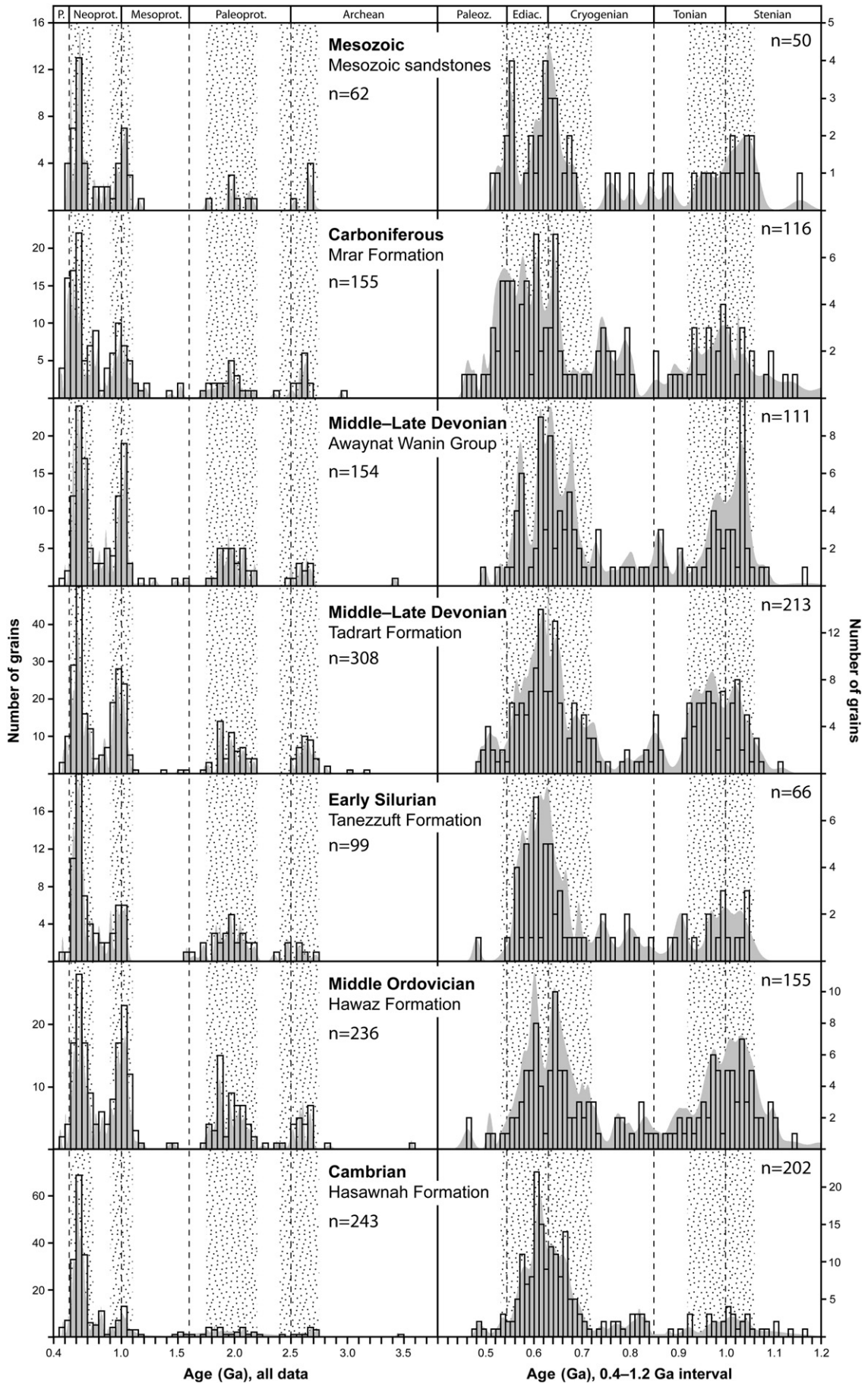
Paleoproterozoic (2200–1800 Ma) and the earliest Proterozoic–Neoproterozoic (2800–2400 Ma) groups resemble the ages of the basement in the cratonic areas of the SMC (Abdelsalam et al., 2002).

The origin of the late Mesoproterozoic to early Neoproterozoic (1200–900 Ma) group is enigmatic, because it has not yet been recognised in the zircon spectra of basement from the SMC (Fig. 3 in Abdelsalam et al., 2002). Küster et al. (2008) recently described ~900–920 Ma-old metamorphic zircons from basement of the Bayuda Desert in Sudan, which indicate an orogenic event preceding the East African Orogeny (as defined by Stern, 1994, and refined by Collins and Pisarevsky, 2005) at the eastern boundary of the Sahara Metacraton. These early Neoproterozoic zircons show Th/U values <0.2. However, in the present study, zircons of such age have Th/U values >0.3 (see Appendix B), which makes detrital input from the eastern SMC unlikely. Interestingly, inherited zircon grains in parts of the Arabian–Nubian Shield (ANS) suggest minor involvement of Mesoproterozoic and older basement or sediment during Neoproterozoic magma ascent (Hargrove et al., 2006) but they cannot account for the high number of detrital zircon grains with pre-900 Ma ages in the sandstones analysed in this study. Be'eri-Shlevin et al. (2009) described U–Pb zircon (1130–930 Ma) ages from the Sa'al schist in Sinai. This, together with the euhedral shape of some of these grains and the lack of other pre-Neoproterozoic zircon ages in the Sa'al schist is taken as evidence for 1.1–0.9 Ga-old crust at the northeastern margin of western Gondwana prior to the formation of the ANS, and thus zircons with such age detected in lower Paleozoic sandstones have a proximal provenance (Be'eri-Shlevin et al., 2009). Detrital zircons from a Neoproterozoic (ca. 740 Ma) diamictite of the Eastern Desert of Egypt (Ali et al., 2010) have similar Neoproterozoic, Paleoproterozoic and Neoproterozoic peaks but a much smaller ca. 1 Ga peak than samples from southern Libya. This may suggest that the ca. 1 Ga source was closer to Libya than to eastern Egypt.

Paleocurrent data from early Paleozoic strata of southern Libya indicate flow roughly from south to north (towards NW–N–NE), which would discount far-field sediment input from the Hoggar in the west and the northern ANS in the east respectively. Furthermore, during the Silurian, a large delta system prograded in a northwesterly direction from the middle Llandovery to the Pridolian (e.g., Craig et al., 2008; Hallett, 2002). Thus, potential source lithologies for the Paleozoic sandstones should be sought in the southern and southeastern part of the SMC or further towards the south and southeast.

The origin of 1200–900 Ma-old zircons in sediments of the eastern Murzuq Basin remains enigmatic, since the nearest recorded igneous basement exposure of that age is located to the south, in eastern Chad (western Dharfur region) where extensive ca. 900 and ca. 600 Ma granitoids, predominantly derived from melting of 3.0–1.0 Ga continental lithosphere, are present (de Wit et al., 2005). This composite continental crust, which is termed the Great Central Saharan Arc, can be traced from the Tibesti Massif through western Darfur and Cameroon into Brazil (de Wit et al., 2005). Further igneous basement exposures of ca. 1 Ga are found at the southeastern edge of the Congo craton in the Irumide Belt of Zambia where voluminous K-rich granitoids intruded at ca. 1050–950 Ma (De Waele et al., 2003, 2009). Note that the Kibaran Belt can be excluded as the source area since this belt records a prominent tectono-magmatic event associated with voluminous bimodal magmatism at ca. 1375 Ma (Tack et al., 2010), which is not recorded in detrital zircon U–Pb ages of this study. The Irumide Belt related to the Irumidian orogeny can be traced along the southeastern margins of the Congo and Tanzania cratons (Bingen et al., 2009).

**Fig. 5.** Histograms and probability density curves show U–Pb analytical zircon data for analysed Paleozoic and Mesozoic sandstones from the eastern Murzuq Basin. Four main age populations (highlighted with dotted shading) are identified in sandstones from the eastern Murzuq Basin (see text for discussion). Histograms and probability density curves for each single sample analysed in this study can be found as Supplementary data (see Appendix B). Only grains with 90 to 110% concordance are shown.  $n$  = number of grains analysed. Note the increase in 920–1060 Ma-old zircons in the Middle Ordovician Hawaz Formation and the increase in <580 Ma-old zircons in the Carboniferous Mrar Formation.



There are two possible explanations for the presence of ca. 1 Ga zircons in the Paleozoic sediments of Dor el Gussa. They could represent primary input, either from the Irumide Belt by long-distance transport, as suggested by Kolodner et al. (2006) for quartz-rich sandstones from Jordan and Israel, or from late Mesoproterozoic and earliest Neoproterozoic granitoids in the SMC. Although such granitoids have not yet been recognised, this could be due to the relatively limited amount of knowledge of the area. Alternatively, the ca. 1 Ga zircons could have been recycled from Neoproterozoic sediments. This hypothesis is based on the occurrence of a prominent zircon population at 1200–950 Ma (18%) in metasediments from the Arkenu Formation of the eastern Kufra Basin, in conjunction with main zircon populations at 3000–2400 Ma (42%) and 2200–1900 Ma (29%) (Fig. 7). The youngest detrital zircon grain is  $951 \pm 11$  Ma (1 $\sigma$ ), which suggests that deposition of the Arkenu Formation took place after ca. 951 Ma but prior to the Cryogenian–Ediacaran orogenic cycle (Le Heron et al., 2009). Interestingly, metasedimentary garnet–cordierite–gneisses at Sabaloka in Sudan contain detrital zircons ranging in age from 2600 to 900 Ma (Kröner et al., 1987), and may therefore represent an equivalent sedimentary deposit to the Arkenu Formation. Furthermore, the Sa'al schist in Sinai, which also contains ca. 1 Ga zircons (Be'eri-Shlevin et al., 2009), may also represent an equivalent sedimentary deposit. If so, a vast amount of Tonian metasediments with 1200–900 Ma-old detrital zircons must exist within the SMC and along its eastern margin. Recycling of these metasediments is a potential source for ca. 1 Ga zircons in Phanerozoic cover sequence (especially first-cycle Cambrian sediments) of the central SMC in southern Libya.

Extending the previous discussion, if the ca. 1 Ga detrital zircons are recycled from Tonian sediments, then their original source may have been a part of a continent that is no longer found in Africa. Such a continent containing ca. 1 Ga igneous rocks may have been attached to the SMC, but rifted off during the break-up of Rodinia in late Tonian–early Cryogenian times. Alternatively, this continent could have been subducted during the assembly of Gondwana in Cryogenian–Ediacaran times.

It is worth pointing out that a prominent input of ca. 1 Ga zircons occurs at some point between the late Cambrian and late Middle Ordovician. About 22% of all zircons in the Hawaz Formation sandstones are dated as 1060–920 Ma, whereas Cambrian Hasawnah Formation sandstones also contain ca. 1-Ga-old zircons but in lesser amount (12% of all zircons are 1060–920 Ma-old) (Fig. 6). The Hasawnah Formation sandstones are likely first-cycle sediments derived

from the Cryogenian–Ediacaran basement, as indicated by the high amount of Cryogenian–Ediacaran zircons (Figs. 5 and 6). The youngest concordant zircon grains in the Hawaz Formation are  $464 \pm 17$  Ma in sample H6063 and  $461 \pm 23$  Ma in sample P5880, giving the maximum age of deposition for the Hawaz Formation as late Middle Ordovician. The increase in ca. 1-Ga-old zircons in the Hawaz Formation as well as the presence of Darriwilian zircons suggests tectonic and magmatic activity during deposition of the Hawaz Formation. Interestingly, several K-bentonite beds have been reported from the Hawaz Formation of western Garga (Fig. 1b), suggesting felsic calc-alkaline volcanism during the Darriwilian (Ramos et al., 2003, 2006), coincident with plate tectonic reorganisations at the peri-Gondwana margin (e.g., Meinhold et al., 2011 and references therein). This causal link certainly needs further studies but this is beyond the scope of the present paper.

The ubiquitous occurrence of ca. 1 Ga zircons in Tonian metasediments and the Phanerozoic cover sequence of the SMC provides insights into the correlation and paleotectonic arrangement of Gondwana-derived terranes, exposed, for example, in SW Turkey (Kröner and Şengör, 1990), the Cyclades (Key and Lister, 2002) and further away in NW Iberia (Fernández-Suárez et al., 2002a,b) where ca. 1 Ga detrital zircons have also been found. Judging from the results of this study, there is no need for margin-parallel dextral terrane transport, as proposed by Fernández-Suárez et al. (2002a,b) to explain the presence of Mesoproterozoic zircons in the Ordovician Armorican quartzite of NW Iberia with derivation from Amazonia. The presence of Mesoproterozoic zircons in terranes of southwestern Europe could also be explained in terms of derivation from the SMC rather than invoking margin-parallel sinistral terrane transport, which would have significant implications for current paleotectonic models (cf. Fernández-Suárez et al., 2002a,b). This hypothesis should certainly be tested further.

There is a distinct change in zircon age populations at the base of the Middle Ordovician Hawaz Formation (Figs. 5 and 6). The Neoproterozoic group dominates the age spectra in the Cambrian Hasawnah Formation, forming 63–77% of the entire zircon population. Only minor amounts of the other three main groups are recognised (Figs. 5 and 6). Such population spectra imply sourcing was dominantly from Cryogenian–Ediacaran basement areas, without much input from older basement rocks. In contrast, the Hawaz Formation, Tanezzuft Formation, Tadrart Formation and Awaynat Wanin Group populations are more diverse, with the 2750–2500 Ma group forming 4–11%, the 2200–1750 Ma group 8–22%, the 1060–920 Ma group 12–23%, the 720–530 Ma group 29–56%, and rare grains >3 Ga.

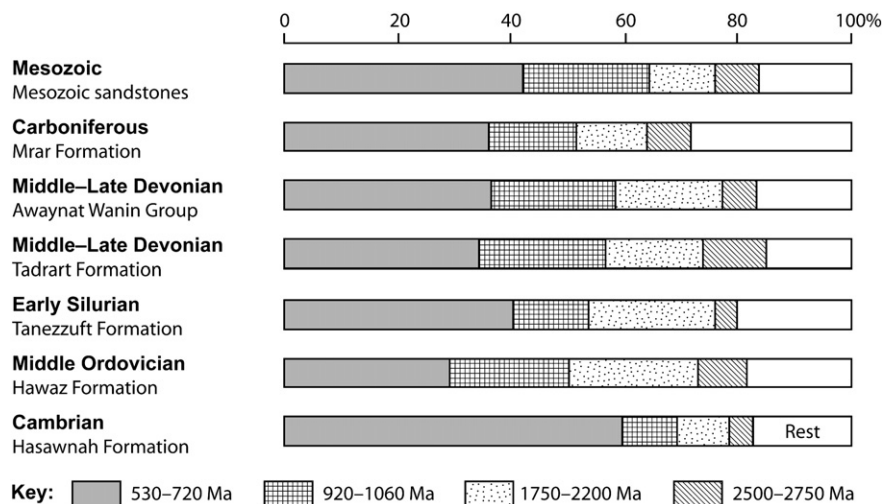
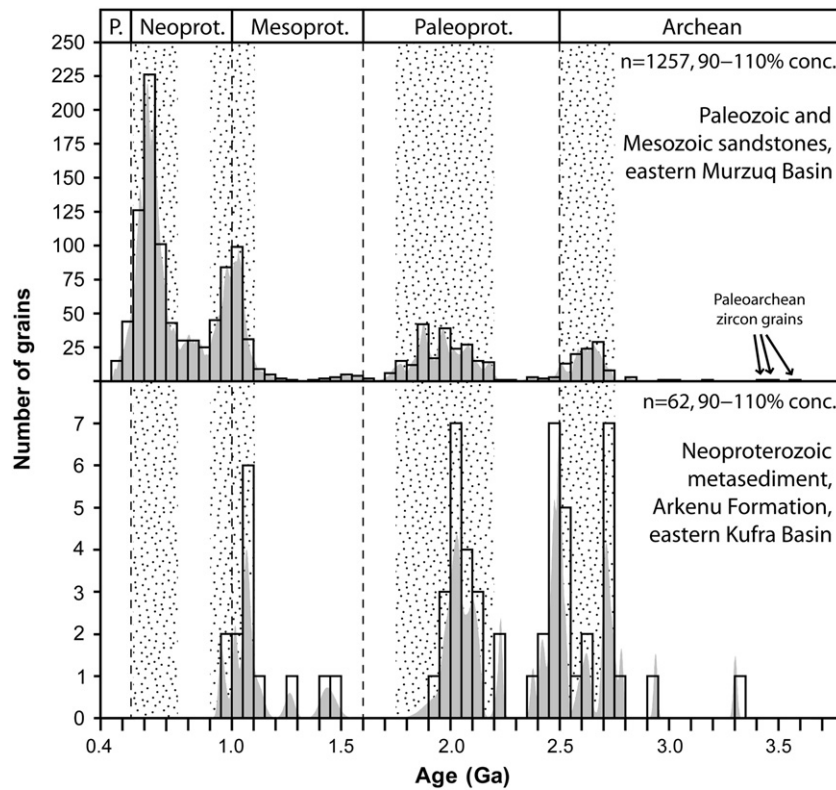


Fig. 6. Relative abundances (%) of detrital zircons in the most prominent age groups identified in sandstones from the eastern Murzuq Basin. Includes all data with 90 to 110% concordance. Note the predominance of 530–720 Ma-old zircons in the Cambrian Hasawnah Formation (first-cycle sediments derived from the Cryogenian–Ediacaran basement) and the increase in 920–1060 Ma-old zircons in the Middle Ordovician Hawaz Formation.



**Fig. 7.** Histograms and probability density curves show summary of U–Pb analytical detrital zircon data for all samples analysed in this study. Four main age populations (highlighted with dotted shading) are identified in sandstones from the eastern Murzuq Basin (see text for discussion). Detrital zircon data from a metasedimentary sample of the Neoproterozoic Arkenu Formation of the eastern Kufra Basin (sample H2519; Le Heron et al., 2009) are shown for comparison (bottom). The Arkenu Formation sample is classified as a sublitharenite, with quartz–feldspar–lithic fragments (Q–F–L) end members of 87–0–13, following the Gazzi–Dickinson method (Ingersoll et al., 1984). The corresponding U–Pb isotopic data are given as Supplementary data (see Appendix B).

A further change in sediment source occurs at the base of the Carboniferous Mrar Formation. Samples from the Mrar Formation are characterised by a small but significant quantity of detrital zircons with ages between 810 and 720 Ma. Zircons with ages <542 Ma (younger than Precambrian) are more common than in older formations (Fig. 5). Furthermore, Mrar Formation sandstones are characterised by high garnet:zircon and rutile:zircon ratios, different to underlying formations (Fig. 4). This change may be related to provenance, but without access to subsurface samples, the possibility that at least some of the pattern is due to variable weathering cannot be entirely discounted (Morton et al., 2011).

Finally, although single grains should be treated cautiously, the early Archean zircon grain of  $3570 \pm 23$  Ma (98% concordance) from the Hawaz Formation (sample H6048) is of great importance for paleo-source characterisation. In North and West Africa, early Archean ages >3.5 Ga have only been reported so far from a migmatitic orthogneiss in northern Nigeria (Kröner et al., 2001), which rivals with the oldest African crustal rock in Swaziland ( $3644 \pm 4$  Ma; Compston and Kröner, 1988). Slightly “younger” ages of ca. 3540 Ma and ca. 3515 Ma are known from basement rocks of Guinea (Kenema–Man Shield) and northern Mauritania (Reguibat Shield) respectively (Potrel et al., 1996; Thiéblemont et al., 2001). However, we do not necessarily suggest that the source is from as far afield as the southwestern part of West Africa. Early Archean crust could have been reworked during younger magmatic events, and thus 3.6–3.5 Ga-old zircons may represent recycled xenocrysts.

## 6. Conclusions

About 75% (1257 grains) of all analysed detrital zircons (1678 grains) from Paleozoic and Mesozoic sandstones of the eastern Murzuq Basin are 90 to 110% concordant. Detrital zircons show four

main age groups (Fig. 7), at 2750–2500 Ma (96 grains; 8%), 2200–1750 Ma (206 grains; 16%), 1060–920 Ma (229 grains; 18%), and 720–530 Ma (498 grains; 39%). About 13% of all concordant grains yields ages of 1600–1000 Ma (Mesoproterozoic). In addition, there are 9 zircon grains (0.7% of all concordant grains) with ages of 3600–2800 Ma (Paleo- and Mesoarchean).

The high numbers of ca. 1 Ga zircons, which have not yet been reported from igneous basement rocks of North Africa, could have been derived from ca. 1 Ga igneous rocks in eastern Chad and ca. 1 Ga igneous rocks along the southeastern margins of the Congo and Tanzania cratons. This is supported by sediment transport directions. Alternatively, the ca. 1 Ga zircons could have been recycled from Neoproterozoic sediments such as the Arkenu Formation or equivalent rocks, which are known to contain zircons of this age. The ubiquitous occurrence of ca. 1 Ga zircons in the Paleozoic and Mesozoic sedimentary sequence of central North Africa provides insights into the correlation and paleotectonic arrangement of Gondwana-derived terranes in SW Europe and the Eastern Mediterranean. Current paleotectonic models of margin-parallel dextral terrane transport may need to be revised (cf. Fernández-Suárez et al., 2002a,b), and should be tested in future studies.

## Acknowledgements

We are very grateful to Y. Abutarruma, R. Aburawi, A.I. Asbali, B. Belgasem, F. Said and B. Thusu for their scientific support and guidance during the project work in Libya. We also would like to thank the logistics team, provided by B. Grenat, for assistance in the field. The administrative and logistical support of staff at the Libyan Petroleum Institute is gratefully acknowledged. The consortium of subscribing oil and gas companies is thanked for its financial support to the CASP Southern Basins of Libya Project. We thank R. Scott for the

internal review of the paper and A.S. Collins and two anonymous referees for their very thorough and insightful journal reviews.

## Appendix A. Sample preparation and analytical techniques

U–Pb isotopic analyses of individual zircon grains were performed either using the sensitive high-resolution ion microprobe (SHRIMP RG) at the Research School of Earth Sciences (RSES), The Australian National University, Canberra, Australia (7 samples), or by laser ablation sector-field inductively-coupled plasma–mass spectrometry (LA-SF-ICP–MS) at the Geological Survey of Denmark and Greenland, Copenhagen, Denmark (12 samples). In both cases, zircons were separated from the heavy mineral concentrates, which were prepared for conventional heavy mineral analysis using standard heavy liquid separation techniques (Morton et al., 2011).

Sample preparation for SHRIMP analysis involved further zircon concentration by paramagnetic methods. The resulting zircon-rich heavy mineral concentrates were poured onto double-sided tape, mounted in epoxy together with chips of the reference zircons (Temora and SL13), sectioned approximately in half, and polished. Reflected and transmitted light photomicrographs and cathodoluminescence (CL) scanning electron microscope (SEM) images were prepared for all zircon grains. The CL images were used to decipher the internal structures of the sectioned grains and to ensure that the ~20 µm SHRIMP spot was wholly within a single age component (usually the youngest) within the sectioned grains.

Each U–Pb isotopic analysis by SHRIMP RG consisted of 4 or 5 scans through the mass range, with a reference zircon analysed for every five unknown zircon analyses. The SHRIMP analytical method follows Williams (1998, and references therein). The data have been reduced using the SQUID Excel Macro of Ludwig (2001). Isoplot/Ex (Ludwig, 2003) was used for age calculations. The U/Pb ratios have been normalised relative to a value of 0.0668 for the Temora reference zircon, equivalent to an age of 417 Ma (see Black et al., 2003). Correction for common Pb was either made using the measured  $^{204}\text{Pb}/^{206}\text{Pb}$  ratio in the normal manner, except for grains younger than ca. 800 Ma (or those low in U and, consequently, radiogenic Pb), where the  $^{207}\text{Pb}$  correction method has been used (see Williams, 1998). Note that when the  $^{207}\text{Pb}$  correction is applied, it is not possible to determine radiogenic  $^{207}\text{Pb}/^{206}\text{Pb}$  ratios or ages.

For LA-SF-ICP–MS analysis, final purification was carried out by hand picking under a binocular microscope. Zircon grains were set in epoxy resin mounts, sectioned and polished to approximately half their original thickness. Prior to analysis, backscatter electron (BSE) images were obtained using a scanning electron microscope (SEM). This allowed the internal structure of the zircons to be examined, enabling the targeting of specific areas for analysis, for example, growth structures and inherited cores.

The U–Pb isotopic analyses were performed using a Thermo-Finnigan Element II sector-field ICPMS system coupled to a Merchantek/NewWave 213 nm Nd-YAG laser system at the Geological Survey of Denmark and Greenland, Copenhagen, Denmark. The zircon mounts were rigorously cleaned in an ultrasonic bath before introducing them into the sample cell to remove surface lead contamination. The method applied essentially followed that described by Frei and Gerdes (2009) and Meinhold et al. (2010a). All data were acquired with single-spot analyses on individual zircon grains using a 30 µm spot size. Long-term precision ( $2\sigma$ ) of the method based on 402 individual analyses of the Plešovice zircon standard (Sláma et al., 2008) is 2.2%, 3.1% and 2.1% for the  $^{206}\text{Pb}/^{238}\text{U}$ ,  $^{207}\text{Pb}/^{235}\text{U}$  and  $^{207}\text{Pb}/^{206}\text{Pb}$  ratios respectively (Frei and Gerdes, 2009). The accuracy and reproducibility of the applied LA-ICP–MS method has recently been tested by Meinhold et al. (2010b) who present U–Pb data on zircon grains previously dated by SHRIMP-II. Furthermore, chips of the TEMORA 1 zircon standard were treated as unknown during the LA-ICP–MS analytical session by Meinhold et al. (2010b).

For the interpretation of the zircon data, analyses with 90–110% concordance (calculated from  $100 \times (^{206}\text{Pb}/^{238}\text{U} \text{ age}) / (^{207}\text{Pb}/^{206}\text{Pb} \text{ age})$ ) are considered to be concordant. Grains with ages >10% discordance and those that gave unreliable isotopic ratios during measurement (e.g., massive common Pb,  $^{238}\text{U}/^{206}\text{Pb}$  fractionation) were rejected and consequently not considered for diagrams and data interpretation. Unless stated otherwise,  $^{206}\text{Pb}/^{238}\text{U}$  ages are used for zircon grains <1.2 Ga whereas older grains are quoted using their  $^{207}\text{Pb}/^{206}\text{Pb}$  ages. This is because the  $^{207}\text{Pb}/^{206}\text{Pb}$  ages become increasingly imprecise below <1.2 Ga due to small amounts of  $^{207}\text{Pb}$ . The  $^{207}\text{Pb}/^{206}\text{Pb}$  ages are generally considered as minimum ages due to the effect of possible Pb loss. For data presentation, histograms and probability density curves were produced using the AgeDisplay program (Sircombe, 2004). Note no concordance could be calculated for zircon grains with a  $^{206}\text{Pb}/^{238}\text{U}$  SHRIMP age <800 Ma because it was not possible to determine radiogenic  $^{207}\text{Pb}/^{206}\text{Pb}$  ratios or ages since for such grains the  $^{207}\text{Pb}$  correction has been applied. Here by convention their age is assumed to be within 90–110% concordance. Unless stated otherwise, ages reported in the text are given at the 2-sigma level. The geological time scale of Ogg et al. (2008) was used as stratigraphic reference for data interpretation.

## Appendix B. Supplementary data

Supplementary data to this article can be found online at doi:10.1016/j.epsl.2011.09.056.

## References

- Abdelsalam, M.G., Liegeois, J.-P., Stern, R.J., 2002. The Saharan Metacraton. *J. Afr. Earth Sci.* 34, 119–136.
- Abdelsalam, M.G., Gao, S.S., Liegeois, J.-P., 2011. Upper mantle structure of the Saharan Metacraton. *J. Afr. Earth Sci.* 60, 328–336.
- Abuhmida, F.H., 2011. Ordovician–Lower Silurian palynology of the Murzuq Basin, southwest Libya. 44th Annual Meeting of the American Association of Stratigraphic Palynologists, 4–7 September 2011, Southampton, United Kingdom.
- Ali, K.A., Stern, R.J., Manton, W.I., Johnson, P.R., Mukherjee, S.K., 2010. Neoproterozoic diamictite in the Eastern Desert of Egypt and Northern Saudi Arabia: evidence of 750 Ma glaciation in the Arabian–Nubian Shield. *Int. J. Earth Sci.* 90, 705–726.
- Avigad, D., Kolodner, K., McWilliams, M., Persing, H., Weissbrod, T., 2003. Origin of northern Gondwana Cambrian sandstone revealed by detrital zircon SHRIMP dating. *Geology* 31, 227–230.
- Aziz, A., 2000. Stratigraphy and hydrocarbon potential of the lower Palaeozoic succession of License NC-115, Murzuq Basin, SW Libya. In: Sola, M.A., Worsley, D. (Eds.), *Geological Exploration in Murzuq Basin*. Elsevier, Amsterdam, pp. 349–368.
- Baumann, A., El Chair, M., Thiedig, F., 1992. Panafrican granites from deep wells of the Murzuq Basin (Fezzan), western Libya. *N. Jb. Geol. Paläont. Mh.* 1, 1–14.
- Be'eri-Shlevin, Y., Katzir, Y., Whitehouse, M.J., Kleinhanns, C.I., 2009. Contribution of pre Pan-African crust to formation of the Arabian Nubian Shield: New secondary ionization mass spectrometry U–Pb and O studies of zircon. *Geology* 37, 899–902.
- Bertrand, J.M.L., Caby, R., 1978. Geodynamic evolution of the Pan-African orogenic belt: a new interpretation of the Hoggar Shield (Algerian Sahara). *Geol. Rundsch.* 67, 357–388.
- Bingen, B., Jacobs, J., Viola, G., Henderson, I.H.C., Skår, Ø., Boyd, R., Thomas, R.J., Solli, A., Key, R.M., Daudi, E.X.F., 2009. Geochronology of the Precambrian crust in the Mozambique Belt of NE Mozambique, and implications for Gondwana assembly. *Precambrian Res.* 170, 231–255.
- Black, R., Liégeois, J.-P., 1993. Cratons, mobile belts, alkaline rocks and continental lithospheric mantle: the Pan-African testimony. *J. Geol. Soc. Lond.* 150, 89–98.
- Black, L.P., Kamo, S.L., Allen, C.M., Aleinikoff, J.N., Davis, D.W., Korsch, R.J., Foudoulis, C., 2003. TEMORA 1: a new zircon standard for Phanerozoic U–Pb geochronology. *Chem. Geol.* 200, 155–170.
- Boote, D.R., Clark-Lowes, D.D., Traut, M.W., 1998. Palaeozoic petroleum systems of North Africa. In: MacGregor, D.S., Moody, R.T.J., Clark-Lowes, D.D. (Eds.), *The Petroleum Geology of North Africa*: Geol. Soc. Lond., Spec. Publ., vol. 132, pp. 7–68.
- Burke, K., MacGregor, D.S., Cameron, N.R., 2003. Africa's petroleum systems: four tectonic 'Aces' in the past 600 million years. In: Arthur, T.J., MacGregor, D.S., Cameron, N.R. (Eds.), *Petroleum Geology of Africa: New Themes and Developing Technologies*: Geol. Soc. Lond., Spec. Publ., vol. 207, pp. 21–60.
- Collins, A.S., Pisarevsky, S.A., 2005. Amalgamating eastern Gondwana: the evolution of the Circum-Indian Orogens. *Earth Sci. Rev.* 71, 229–270.
- Collomb, G.R., 1962. Carte géologique du Fezzan Oriental, 1:500 000. Compagnie Française des Pétroles, Paris.
- Compston, W., Kröner, A., 1988. Multiple zircon growth within Early Archaean tonalitic gneiss from the Ancient Gneiss Complex, Swaziland. *Earth Planet. Sci. Lett.* 87, 13–28.

- Craig, J.L., Rizzi, C., Said, F., Thusu, B., Lüning, S., Asbali, A.I., Keeley, M.L., Bell, J.F., Durham, M.J., Eales, M.H., Beswetherick, S., Hamblett, C., 2008. Structural styles and prospectivity in the Precambrian and Palaeozoic hydrocarbon systems of North Africa. In: Salem, M.J., Oun, K.M., Essed, A.S. (Eds.), *The Geology of East Libya*, vol. 4. Gutenberg Press, Malta, pp. 51–122.
- Davidson, L., Beswetherick, S., Craig, J., Eales, M., Fisher, A., Himmali, A., Jhoon, J., Mejrab, B., Smart, J., 2000. The structure, stratigraphy and petroleum geology of the Murzuq Basin, southwest Libya. In: Sola, M.A., Worsley, D. (Eds.), *Geological Exploration in Murzuq Basin*. Elsevier, Amsterdam, pp. 295–320.
- De Gibert, J.M., Ramos, E., Marzo, M., 2011. Trace fossils and depositional environments in the Hawaz Formation, Middle Ordovician, western Libya. *J. Afr. Earth Sci.* 60, 28–37.
- De Waele, B., Wingate, M.T.D., Mapani, B., Fitzsimons, I.C.W., 2003. Untying the Kibaran knot: a reassessment of Mesoproterozoic correlations in southern Africa based on SHRIMP U–Pb data from the Irumide belt. *Geology* 31, 509–512.
- De Waele, B., Fitzsimons, I.C.W., Wingate, M.T.D., Tembo, F., Mapani, B., Belousova, E.A., 2009. The geochronological framework of the Irumide Belt: a prolonged crustal history along the margin of the Bangweulu Craton. *Am. J. Sci.* 309, 132–187.
- De Wit, M.J., Bowring, S.A., Dudas, F., Kamga, G., 2005. The great Neoproterozoic central Saharan Arc and the amalgamation of the North African Shield. *GAC-MAC-CSPG-CSSS Joint Meeting, Halifax, Nova Scotia: Abstracts*, 30, pp. 42–43.
- El-Hawat, A.S., Bezan, A., Obeidi, A., Barghathi, H., 2003. The Upper Ordovician–Lower Silurian succession of western Libya: sequence stratigraphy and glacioeustatic-tectonic scenario. In: Salem, M.J., Oun, K.M. (Eds.), *The Geology of Northwest Libya*, vol. 1. Gutenberg Press, Malta, pp. 65–78.
- Fedo, C.M., Sircombe, K.N., Rainbird, R.H., 2003. Detrital zircon analysis of the sedimentary record. In: Hanchar, J.M., Hoskin, P.O. (Eds.), *Zircon: Rev. Mineral. Geochem.*, vol. 53, pp. 277–303.
- Fernández-Suárez, J., Gutiérrez-Alonso, G., Cox, R., Jenner, G.A., 2002a. Assembly of the Armorican microplate: a strike-slip terrane delivery? Evidence from U–Pb ages of detrital zircons. *J. Geol.* 110, 619–626.
- Fernández-Suárez, J., Gutiérrez-Alonso, G., Jeffries, T.E., 2002b. The importance of along-margin terrane transport in northern Gondwana: insights from detrital zircon parentage in Neoproterozoic rocks from Iberia and Brittany. *Earth Planet. Sci. Lett.* 204, 75–88.
- Frei, D., Gerdes, A., 2009. Precise and accurate in situ U–Pb dating of zircon with high sample throughput by automated LA–SF–ICP–MS. *Chem. Geol.* 261, 261–270.
- Ghuma, M.A., Rogers, J.J.W., 1978. Geology, geochemistry, and tectonic setting of the Ben Ghema batholith, Tibesti massif, southern Libya. *Geol. Soc. Am. Bull.* 89, 1351–1358.
- Hallett, D., 2002. *Petroleum Geology of Libya*. Elsevier, Amsterdam, pp. 1–503.
- Hargrove, U.S., Stern, R.J., Kimura, J.-I., Manton, W.I., Johnson, P.R., 2006. How juvenile is the Arabian–Nubian Shield? Evidence from Nd isotopes and pre-Neoproterozoic inherited zircon in the Bi'r Umq suture zone, Saudi Arabia. *Earth Planet. Sci. Lett.* 252, 308–326.
- Hohndorf, A., Meinhold, K.D., Vail, J.R., 1994. Geochronology of anorogenic igneous complexes in the Sudan— isotopic investigations in north Kordofan, the Nubian Desert and the Red-Sea Hills. *J. Afr. Earth Sci.* 19, 3–15.
- Ingersoll, R.V., Bullard, T.F., Ford, R.L., Grimm, J.P., Pickle, J.P., Sares, S.W., 1984. The effect of grain size on detrital modes: a test of the Gazzi–Dickinson Point Counting method. *J. Sed. Petrol.* 54, 103–116.
- Johnson, P.R., Andresen, A., Collins, A.S., Fowler, A.R., Fritz, H., Ghebreab, W., Kusky, T., Stern, R.J., 2011. Late Cryogenian–Ediacaran history of the Arabian–Nubian Shield: a review of depositional, plutonic, structural, and tectonic events in the closing stages of the northern East African Orogen. *J. Afr. Earth Sci.* 61, 167–232.
- Keay, S., Lister, G.S., 2002. African provenance for the metasediments and metaigneous rocks of the Cyclades, Aegean Sea. *Geology* 30, 235–238.
- Key, R., 1992. An introduction to the crystalline basement of Africa. In: Wright, E., Burgess, W. (Eds.), *Hydrogeology of Crystalline Basement Aquifers in Africa: Geol. Soc. Lond., Spec. Publ.*, vol. 66, pp. 29–57.
- Klitzsch, E., 1964. Zur Geologie am Ostrand des Murzukbeckens (Provinz Fezzan, Libyen). *Oberrhein. Geol. Abh.* 13, 51–73.
- Klitzsch, E., Ziegert, H., 2000. Short notes and guidebook on the geology of the Dor el Gussa – Jabal Bin Ghanimah area. *Sedimentary Basins of Libya, Second Symposium, Geology of Northwest Libya*. Gutenberg Press, Malta, pp. 1–52.
- Kolodner, K., Avigad, D., McWilliams, M., Wooden, J.L., Weissbrod, T., Feinstein, S., 2006. Provenance of north Gondwana Cambrian–Ordovician sandstone: U–Pb SHRIMP dating of detrital zircons from Israel and Jordan. *Geol. Mag.* 143, 367–391.
- Kröner, A., Şengör, A.M.C., 1990. Archean and Proterozoic ancestry in late Precambrian and early Paleozoic crustal elements in southern Turkey as revealed by single zircon dating. *Geology* 18, 1186–1190.
- Kröner, A., Stern, R.J., Dawoud, A.S., Compston, W., Reischmann, T., 1987. The Pan-African continental margin in northeastern Africa: evidence from a geochronological study of granulites at Sabaloka, Sudan. *Earth Planet. Sci. Lett.* 85, 91–104.
- Kröner, A., Ekwueme, B.N., Pidgeon, R.T., 2001. The oldest rocks in West Africa: SHRIMP zircon age for Early Archean magmatic orthogneiss at Kaduna, northern Nigeria. *J. Geol.* 109, 399–406.
- Küster, D., Liégeois, J.-P., Matukov, D., Sergeev, S., Lucassen, F., 2008. Zircon geochronology and Sr, Nd, Pb isotope geochemistry of granitoids from Bayuda Desert and Sabaloka (Sudan): evidence for a Bayudian event (920–900 Ma) preceding the Pan-African orogenic cycle (860–590 Ma) at the eastern boundary of the Saharan Metacraton. *Precambrian Res.* 164, 16–39.
- Le Heron, D.P., Sutcliffe, O.E., Whittington, R.J., Craig, J., 2005. The origins of glacially related soft-sediment deformation structures in Upper Ordovician glaciogenic rocks: implication for ice sheet dynamics. *Palaeogeogr. Palaeoclimat. Palaeoecol.* 218, 75–103.
- Le Heron, D.P., Howard, J.P., Alhassi, A.M., Anderson, L.M., Morton, A.C., Fanning, C.M., 2009. Field-based investigations of an ‘Infracambrian’ clastic succession in SE Libya and its bearing on the evolution of the Al Kufrah Basin. In: Craig, J., Thurow, J., Thusu, B., Whitham, A.G., Abutarruma, Y. (Eds.), *Global Neoproterozoic Petroleum Systems: The Emerging Potential in North Africa: Geol. Soc. Lond., Spec. Publ.*, vol. 326, pp. 193–210.
- Ludwig, K.R., 2001. *SQUID 1.00, a User's Manual*. Berkeley Geochronology Center. Spec. Publ. 2.
- Ludwig, K.R., 2003. *Isoplot/Ex version 3.0: A Geochronological Toolkit for Microsoft Excel*. Berkeley Geochronology Center. Spec. Publ. 4.
- McDougall, N., Martin, M., 2000. Facies models and sequence stratigraphy of Upper Ordovician outcrops in the Murzuq Basin, SW Libya. In: Sola, M.A., Worsley, D. (Eds.), *Symposium on Geological Exploration in Murzuq Basin*. Elsevier, Amsterdam, pp. 223–236.
- Meinhold, G., Frei, D., 2008. Detrital zircon ages from the islands of Inousses and Psara, Aegean Sea, Greece: constraints on depositional age and provenance. *Geol. Mag.* 145, 886–891.
- Meinhold, G., Kostopoulos, D., Frei, D., Himmerkus, F., Reischmann, T., 2010a. U–Pb LA–SF–ICP–MS zircon geochronology of the Serbo-Macedonian Massif, Greece: palaeotectonic constraints for Gondwana-derived terranes in the Eastern Mediterranean. *Int. J. Earth Sci.* 99, 813–832.
- Meinhold, G., Reischmann, T., Kostopoulos, D., Frei, D., Larionov, A.N., 2010b. Mineral chemical and geochronological constraints on the age and provenance of the eastern Circum-Rhodope Belt low-grade metasedimentary rocks, NE Greece. *Sed. Geol.* 229, 207–223.
- Meinhold, G., Arslan, A., Lehnert, O., Stampfli, G.M., 2011. Global mass wasting during the Middle Ordovician: meteoritic trigger or plate-tectonic environment? *Gondwana Res.* 19, 535–541.
- Mergl, M., Massa, D., 2000. A palaeontological review of the Devonian and Carboniferous succession of the Murzuq Basin and the Djado Sub-Basin. In: Sola, M.A., Worsley, D. (Eds.), *Geological Exploration in Murzuq Basin*. Elsevier, Amsterdam, pp. 41–88.
- Morton, A.C., Meinhold, G., Howard, J.P., Phillips, R.J., Strogen, D., Abutarruma, Y., Elgady, M., Thusu, B., Whitham, A.G., 2011. A heavy mineral study of sandstones from the eastern Murzuq Basin, Libya: Constraints on provenance and stratigraphic correlation. *J. Afr. Earth Sci.* doi:10.1016/j.jafrearsci.2011.08.005.
- Ogg, J.G., Ogg, G., Gradstein, F.M., 2008. *The Concise Geologic Time Scale*. Cambridge University Press, p. 177.
- Pegram, B.J., Register, J.K., Fullagar, P.D., Ghuma, M.A., Rogers, J.J.W., 1976. Pan-African ages from a Tibesti massif batholith, southern Libya. *Earth Planet. Sci. Lett.* 30, 123–128.
- Persits, F.M., Ahlbrandt, T.S., Tuttle, M.L., Charpentier, R.R., Brownfield, M.E., Takahashi, K.I., 2002. Maps showing geology, oil and gas fields, and geological provinces of Africa. *U.S. Geological Survey*.
- Potrel, A., Peucat, J.J., Fanning, C.M., Auvray, B., Burg, J.P., Caruba, C., 1996. 3.5 Ga old terranes in the West African Craton, Mauretania. *J. Geol. Soc. Lond.* 153, 507–510.
- Ramos, E., Navidad, M., Marzo, M., Bolatti, N., 2003. Middle Ordovician K-bentonite beds in the Murzuq Basin (Central Libya). In: Albanesi, G.L., Beresi, M.S., Peralta, S.H. (Eds.), *Ordovician from the Andes: Instituto Superior de Correlación Geológica*, vol. 17, pp. 203–207.
- Ramos, E., Marzo, M., de Gibert, J.M., K.S., T., Khoja, A.A., Bolatti, N.D., 2006. Stratigraphy and sedimentology of the Middle Ordovician Hawaz Formation (Murzuq Basin, Libya). *AAPG Bulletin* 90, 1309–1336.
- Sircombe, K.N., 2004. *AgeDisplay: an EXCEL workbook to evaluate and display univariate geochronological data using binned frequency histograms and probability density distributions*. *Comput. Geosci.* 30, 21–31.
- Sláma, J., Košler, J., Condon, D.J., Crowley, J.L., Gerdes, A., Hanchar, J.M., Horstwood, M.S.A., Morris, G.A., Nasdala, L., Norberg, N., Schaltegger, U., Schoene, B., Tubrett, M.N., Whitehouse, M.J., 2008. Plešovice zircon – a new natural reference material for U–Pb and Hf isotopic microanalysis. *Chem. Geol.* 249, 1–35.
- Stern, R.J., 1994. Arc assembly and continental collision in the Neoproterozoic East African Orogen: implications for the assembly of Gondwanaland. *Ann. Rev. Earth Planet. Sci.* 22, 319–351.
- Tack, L., Wingate, M.T.D., De Waele, B., Meert, J., Belousova, E., Griffin, B., Tahon, A., Fernández-Alonso, M., 2010. The 1375 Ma “Kibaran event” in Central Africa: prominent emplacement of bimodal magmatism under extensional regime. *Precambrian Res.* 180, 63–84.
- Thiéblemont, D., Delor, C., Cocherie, A., Lafon, J.M., Goujou, J.C., Baldé, A., Bah, M., Sané, H., Fanning, M., 2001. A 3.5 Ga granite–gneiss basement in Guinea: further evidence for early Archean accretion within the West African Craton. *Precambrian Res.* 108, 179–194.
- Veevers, J.J., 2007. Pan-Gondwanaland post-collisional extension marked by 650–500 Ma alkaline rocks and carbonatites and related detrital zircons: a review. *Earth Sci. Rev.* 83, 1–47.
- Williams, I.S., 1998. U–Th–Pb geochronology by ion microprobe. In: McKibben, M.A., Shanks III, W.C., Ridley, W.I. (Eds.), *Applications of microanalytical techniques to understanding mineralising processes: Reviews in Economic Geology*, vol. 7, pp. 1–35.